TECHNICAL SPECIFICATION

ISO/TS 6336-20

Second edition
2022-05

Calculation of load capacity of spur and helical gears —

Part 20: Calculation of scuffing load capacity — Flash temperature method

Calcul de la capacité de charge des engrenages cylindriques à dentures droite et hélicoïdale —

Partie 20: Calcul de la capacité de charge au grippage — Méthode de la température-éclair

Reference number
ISO/TS 6336-20:2022(E)

ISO copyright office
CP 401 • Ch. de Blandonnet 8
CH-1214 Vernier, Geneva
Phone: +41 22 749 01 11
Email: copyright@iso.org
Website: www.iso.org

Published in Switzerland

Contents

Page

Foreword

ISO (the International Organization for Standardization) is a worldwide federation of national standards bodies (ISO member bodies). The work of preparing International Standards is normally carried out through ISO technical committees. Each member body interested in a subject for which a technical committee has been established has the right to be represented on that committee. International organizations, governmental and non-governmental, in liaison with ISO, also take part in the work. ISO collaborates closely with the International Electrotechnical Commission (IEC) on all matters of electrotechnical standardization.

The procedures used to develop this document and those intended for its further maintenance are described in the ISO/IEC Directives, Part 1. In particular, the different approval criteria needed for the different types of ISO documents should be noted. This document was drafted in accordance with the editorial rules of the ISO/IEC Directives, Part 2 (see www.iso.org/directives).

Attention is drawn to the possibility that some of the elements of this document may be the subject of patent rights. ISO shall not be held responsible for identifying any or all such patent rights. Details of any patent rights identified during the development of the document will be in the Introduction and/or on the ISO list of patent declarations received (see www.iso.org/patents).

Any trade name used in this document is information given for the convenience of users and does not constitute an endorsement.

For an explanation of the voluntary nature of standards, the meaning of ISO specific terms and expressions related to conformity assessment, as well as information about ISO's adherence to the World Trade Organization (WTO) principles in the Technical Barriers to Trade (TBT), see www.iso.org/iso/foreword.html.

This document was prepared by Technical Committee ISO/TC 60, *Gears*, Subcommittee SC 2, *Gear capacity calculation*.

This second edition cancels and replaces the first edition (ISO/TS 6336-20:2017), which has been technically revised.

The main changes are as follows:

— bevel gear related content has been removed after the publication of ISO/TS 10300-20:2021 which precisely covers bevel gears;

— unit of the thermo-elastic factor, X_M, has been corrected in 5.2 and A.4;

— Formula (30) to calculate the parameter on the line of action at point D, Γ_D, has been revised;

— Formula (A.10) to calculate the reduced modulus of elasticity, E_r, has been corrected;

— Formulae (A.11) and (A.12) to calculate the thermal contact coefficients, B_{M1} and B_{M2}, have been corrected;

— Bibliography has been updated.

A list of all parts in the ISO 6336 series can be found on the ISO website.

Any feedback or questions on this document should be directed to the user's national standards body. A complete listing of these bodies can be found at www.iso.org/members.html.

Introduction

The ISO 6336 series consists of International Standards, Technical Specifications (TS) and Technical Reports (TR) under the general title Calculation of load capacity of spur and helical gears (see Table 1).

— International Standards contain calculation methods that are based on widely accepted practices and have been validated.

— TS contain calculation methods that are still subject to further development.

— TR contain data that is informative, such as example calculations.

The procedures specified in ISO 6336-1 to ISO 6336-19 cover fatigue analyses for gear rating. The procedures described in ISO 6336-20 to ISO 6336-29 are predominantly related to the tribological behaviour of the lubricated flank surface contact. ISO 6336-30 to ISO 6336-39 include example calculations. The ISO 6336 series allows the addition of new parts under appropriate numbers to reflect knowledge gained in the future.

Requesting standardized calculations according to ISO 6336 without referring to specific parts requires the use of only those parts that are currently designated as International Standards (see Table 1 for listing). When requesting further calculations, the relevant part or parts of ISO 6336 need to be specified. The use of a technical specification as acceptance criteria for a specific design needs to be agreed in advance between the manufacturer and the purchaser.

Table 1 — Overview of ISO 6336

Calculation of load capacity of spur and helical gears	International Standard	Technical Specification	Technical Report
Part 1: *Basic principles, introduction and general influence factors*	X		
Part 2: *Calculation of surface durability (pitting)*	X		
Part 3: *Calculation of tooth bending strength*	X		
Part 4: *Calculation of tooth flank fracture load capacity*		X	
Part 5: *Strength and quality of materials*	X		
Part 6: *Calculation of service life under variable load*	X		
Part 20: *Calculation of scuffing load capacity — Flash temperature method*		X	
Part 21: *Calculation of scuffing load capacity — Integral temperature method*		X	
Part 22: Calculation of micropitting load capacity (replaces ISO/TR 15144-1)		X	
Part 30: Calculation examples for the application of *ISO 6336 parts 1,2,3,5*			X
Part 31: Calculation examples of micropitting load capacity (replaces ISO/TR 15144-2)			X
At the time of publication of this document, some of the parts listed here were under development. Consult the ISO website.			

Since 1990, the flash temperature method has been enriched with research for short exposure times, consideration of transition diagrams, new approximations for the coefficient of friction, and completely renewed load sharing factors.

The integral temperature, presented in ISO/TS 6336-21, averages the flash temperature and supplements empirical influence factors to the hidden load sharing factor. The resulting value approximates the maximum contact temperature, thus yielding about the same assessment of scuffing risk as the flash temperature method of this document. The integral temperature method is less sensitive for those cases where there are local temperature peaks, usually in gearsets that have low contact ratio or contact near the base circle or other sensitive geometries.

The risk of scuffing damage varies with the properties of gear materials, the lubricant used, the surface roughness of tooth flanks, the sliding velocities and the load. In contrast to the relatively long time of development of fatigue damage, one single momentary overload can initiate scuffing damage of such severity that affected gears may no longer be used. According to Blok[8][9][10][11][12][13], high contact temperatures of lubricant and tooth surfaces at the instantaneous contact position can effect a breakdown of the lubricant film at the contact interface.

The interfacial contact temperature is conceived as the sum of two components.

— The interfacial bulk temperature of the moving interface, which, if varying, does so only comparatively slowly. The bulk temperature, θ_M, is the equilibrium temperature of the surface of the gear teeth before they enter the contact zone. For evaluating this component, it can be suitably averaged from the two overall bulk temperatures of the two rubbing teeth. The latter two bulk temperatures follow from the thermal network theory[17].

— The rapidly fluctuating flash temperature of the moving faces in contact. The flash temperature is the calculated increase in gear tooth surface temperature at a given point along the path of contact resulting from the combined effects of gear tooth geometry, load, friction, velocity and material properties during operation. The coefficient of friction can significantly influence the result and it is recommended to closely pay attention to its calculation. A common practice is the use of a coefficient of friction valid for regular working conditions, although it can be stated that at incipient scuffing, the coefficient of friction has significantly higher values.

The complex relationship between mechanical, hydrodynamical, thermodynamical and chemical phenomena has been the object of extensive research and experiment. Experimental investigations can induce empirical influence factors. A direct substitution of empirical influence factors can enforce the related functional factors in the main formula to be fixated to average values. However, correct treatment of functional factors (e.g. coefficient of friction, load sharing factor, thermal contact coefficient) keeps the main formula intact, in confirmation with the experiments and practice.

Next to the maximum contact temperature, the progress of the contact temperature along the path of contact provides necessary information to the gear design.

Calculation of load capacity of spur and helical gears —

Part 20: Calculation of scuffing load capacity — Flash temperature method

1 Scope

This document specifies methods and formulae for evaluating the risk of scuffing, based on Blok's contact temperature concept.

The fundamental concept is applicable to all machine elements with moving contact zones. The flash temperature formulae are valid for a band-shaped or approximately band-shaped Hertzian contact zone and working conditions characterized by sufficiently high Péclet numbers.

2 Normative references

The following documents are referred to in the text in such a way that some or all of their content constitutes requirements of this document. For dated references, only the edition cited applies. For undated references, the latest edition of the referenced document (including any amendments) applies.

ISO 1122-1, *Vocabulary of gear terms — Part 1: Definitions related to geometry*

ISO 1328-1, *Cylindrical gears — ISO system of flank tolerance classification — Part 1: Definitions and allowable values of deviations relevant to flanks of gear teeth*

ISO 6336-1, *Calculation of load capacity of spur and helical gears — Part 1: Basic principles, introduction and general influence factors*

ISO 10825, *Gears — Wear and damage to gear teeth — Terminology*

3 Terms and definitions

3.1 Terms and definitions

For the purposes of this document, the terms and definitions given in ISO 1122-1 and ISO 10825 apply.

ISO and IEC maintain terminology databases for use in standardization at the following addresses:

— ISO Online browsing platform: available at https://www.iso.org/obp

— IEC Electropedia: available at https://www.electropedia.org/

3.2 Symbols and units

The symbols used in the formulae are shown in Table 2. The units of length, metre, millimetre and micrometre, have been chosen in accordance with common practice. To achieve a "coherent" system, the units for B_M, c_γ and X_M have been adapted to the mixed application of metre and millimetre or millimetre and micrometre.

NOTE The term *wheel* is used for the mating gear of a pinion.

Table 2 — Symbols and units

Symbol	Description	Unit
A	Tolerance class in accordance with ISO 1328-1	—
a	Centre distance	mm
B_M	Thermal contact coefficient	$N/(mm^{1/2}{\cdot}m^{1/2}{\cdot}s^{1/2}{\cdot}K)$
B_{M1}	Thermal contact coefficient of pinion	$N/(mm^{1/2}{\cdot}m^{1/2}{\cdot}s^{1/2}{\cdot}K)$
B_{M2}	Thermal contact coefficient of wheel	$N/(mm^{1/2}{\cdot}m^{1/2}{\cdot}s^{1/2}{\cdot}K)$
b	Facewidth, smaller value for pinion or wheel	mm
b_H	Semi-width of Hertzian contact band	mm
C_{a1}	Tip relief of pinion	µm
C_{a2}	Tip relief of wheel	µm
C_{eff}	Optimal tip relief	µm
C_{eq1}	Equivalent tip relief of pinion	µm
C_{eq2}	Equivalent tip relief of wheel	µm
C_{f1}	Root relief of pinion	µm
C_{f2}	Root relief of wheel	µm
c_{M1}	Specific heat per unit mass of pinion	J/(kg·K)
c_{M2}	Specific heat per unit mass of wheel	J/(kg·K)
c_γ	Mesh stiffness	N/(mm·µm)
d_{a1}	Tip diameter of pinion	mm
d_{a2}	Tip diameter of wheel	mm
d_1	Reference diameter of pinion	mm
d_2	Reference diameter of wheel	mm
E_1	Modulus of elasticity of pinion	N/mm^2
E_2	Modulus of elasticity of wheel	N/mm^2
E_r	Reduced modulus of elasticity	N/mm^2
F_{ex}	External axial force	N
F_n	Normal load in wear test	N
F_t	Nominal tangential force	N
H_1	Auxiliary dimension	mm
H_2	Auxiliary dimension	mm
K_A	Application factor	—
$K_{B\alpha}$	Transverse load factor (scuffing)	—
$K_{B\beta}$	Face load factor (scuffing)	—
$K_{H\alpha}$	Transverse load factor (contact stress)	—
$K_{H\beta}$	Face load factor (contact stress)	—
K_{mp}	Multiple path factor	—
K_v	Dynamic factor	—
m_n	Normal module	mm
n_p	Number of mesh contacts	—
n_1	Revolutions per minute of pinion	min^{-1}
$Pé_1$	Péclet number of pinion material	—
$Pé_2$	Péclet number of wheel material	—
Ra_1	Tooth flank surface roughness of pinion	µm
Ra_2	Tooth flank surface roughness of wheel	µm
S_B	Safety factor for scuffing	—

Table 2 *(continued)*

Symbol	Description	Unit
S_{FZG}	Load stage (in FZG test)	—
t_c	Contact exposure time at bend of curve	µs
t_{max}	Longest contact exposure time	µs
t_1	Contact exposure time of pinion	µs
t_2	Contact exposure time of wheel	µs
u	Gear ratio	—
u_v	Virtual ratio	—
v_g	Sliding velocity	m/s
v_{g1}	Tangential velocity of pinion	m/s
v_{g2}	Tangential velocity of wheel	m/s
$v_{g\Sigma C}$	Sum of tangential velocities in pitch point	m/s
v_t	Pitch line velocity	m/s
w_{Bn}	Normal unit load	N/mm
w_{Bt}	Transverse unit load	N/mm
$X_{but,\Gamma}$	Buttressing factor	—
$X_{but,A}$	Buttressing value	—
$X_{but,E}$	Buttressing value	—
X_G	Geometry factor	—
X_J	Approach factor	—
X_L	Lubricant factor	—
X_M	Thermo-elastic factor	$K{\cdot}N^{-3/4}{\cdot}s^{1/2}{\cdot}m^{-1/2}{\cdot}mm$
X_{mp}	Multiple mating pinion factor	—
X_R	Roughness factor	—
X_S	Lubrication system factor	—
X_W	Structural factor	—
$X_{\alpha\beta}$	Angle factor	—
X_Γ	Load sharing factor	—
X_Θ	Gradient of the scuffing temperature	—
z_1	Number of teeth of pinion	—
z_2	Number of teeth of wheel	—
α_{a1}	Transverse tip pressure angle of pinion	°
α_{a2}	Transverse tip pressure angle of wheel	°
α_t	Transverse pressure angle	°
α_{wn}	Normal working pressure angle	°
α_{wt}	Transverse working pressure angle	°
α_{y1}	Pinion pressure angle at arbitrary point	°
β	Helix angle	°
β_b	Base helix angle	°
β_w	Working helix angle	°
Γ_A	Parameter on the line of action at point A	—
Γ_{AA}	Parameter on the line of action at point AA	—
Γ_{AB}	Parameter on the line of action at point AB	—
Γ_{AU}	Parameter on the line of action at point AU	—
Γ_B	Parameter on the line of action at point B	—

Table 2 *(continued)*

Symbol	Description	Unit
Γ_{BB}	Parameter on the line of action at point BB	—
Γ_{D}	Parameter on the line of action at point D	—
Γ_{DD}	Parameter on the line of action at point DD	—
Γ_{DE}	Parameter on the line of action at point DE	—
Γ_{E}	Parameter on the line of action at point E	—
Γ_{EE}	Parameter on the line of action at point EE	—
Γ_{EU}	Parameter on the line of action at point EU	—
Γ_{M}	Parameter on the line of action at point M	—
Γ_{y}	Parameter on the line of action at arbitrary point	—
γ_1	Angle of direction of tangential velocity of pinion	
γ_2	Angle of direction of tangential velocity of wheel	—
ε_α	Transverse contact ratio	—
ε_β	Overlap ratio	—
ε_γ	Total contact ratio	—
η_{oil}	Absolute (dynamic) viscosity at oil temperature	mPa·s
Θ_{B}	Contact temperature	°C
Θ_{Bmax}	Maximum contact temperature	°C
Θ_{fl}	Flash temperature	K
Θ_{flm}	Average flash temperature	K
Θ_{flmax}	Maximum flash temperature	K
Θ_{flmaxT}	Maximum flash temperature at test	K
Θ_{M}	Bulk temperature	°C
Θ_{Mi}	Interfacial bulk temperature	°C
Θ_{MT}	Bulk temperature at test	°C
Θ_{M1}	Bulk temperature of pinion teeth	°C
Θ_{M2}	Bulk temperature of wheel teeth	°C
Θ_{oil}	Oil temperature before reaching the mesh	°C
Θ_{S}	Scuffing temperature	°C
Θ_{Sc}	Scuffing temperature at long contact time	°C
λ_{M1}	Heat conductivity of pinion	N/(s·K)
λ_{M2}	Heat conductivity of wheel	N/(s·K)
μ	Coefficient of friction in pin-and-ring test	—
μ_{m}	Mean coefficient of friction	—
ν_1	Poisson's ratio of pinion material	—
ν_2	Poisson's ratio of wheel material	—
ρ_{M1}	Density of pinion material	kg/m^3
ρ_{M2}	Density of wheel material	kg/m^3
ρ_{relC}	Transverse relative radius of curvature at pitch point	mm
ρ_{y1}	Radius of curvature at arbitrary point of pinion	mm
ρ_{y2}	Radius of curvature at arbitrary point of wheel	mm
ρ_{rely}	Relative radius of curvature at arbitrary point y	mm
Φ	Quill shaft twist	°

4 Scuffing and wear

4.1 Occurrence of scuffing and wear

When gear teeth are completely separated by a full fluid film of lubricant, there is no contact between the asperities of the tooth surfaces, and usually, there is no scuffing or wear. Here, the coefficient of friction is rather low. In exceptional cases, a damage similar to scuffing can be caused by a sudden thermal instability[15] in a thick oil film. This phenomenon is not treated here.

For thinner elastohydrodynamic films, incidental asperity contact takes place. Accordingly, as the mean film thickness decreases, the number of contacts increases. Abrasive wear, adhesive wear or scuffing becomes possible. Abrasive wear can occur due to the rolling action of the gear teeth or the presence of abrasive particles in the lubricant. Adhesive wear occurs by localized welding and subsequent detachment and transfer of particles from one or both of the meshing teeth. Abrasive or adhesive wear may not be harmful if it is mild and if it subsides with time, as in a normal run-in process.

In contrast to mild wear, scuffing is a severe form of adhesive wear that can result in progressive damage to the gear teeth. In contrast to pitting and fatigue breakage which show a distinct incubation period, a short transient overloading can result in scuffing failure.

Excessive aeration or the presence in the lubricant of contaminants such as metal particles in suspension, or water, also increases the risk of scuffing damage. After scuffing, high-speed gears tend to suffer high levels of dynamic loading due to vibration which usually cause further damage by scuffing, pitting or tooth breakage.

In most cases, the resistance of gears to scuffing can be improved by using a lubricant with enhanced anti-scuff additives.

NOTE The less correct designation Extreme Pressure (EP) is replaced by anti-scuff.

It is important to be aware that the use of anti-scuff additives can equally lead to some disadvantages, e.g. corrosion of copper, embrittlement of elastomers, lack of world-wide availability.

The methods described are not suitable for “cold scuffing” which is in general associated with low speed, under approximately 4 m/s, through hardened heavily loaded gears of rather poor quality.

4.2 Transition diagram

The lubrication condition of sliding concentrated steel contacts, which operate in a liquid lubricant, can be described[16][17][18][19] in terms of transition diagrams. A transition diagram, according to Figure 1, is considered to be applicable to contacts functioning at constant oil bath temperature.

At combinations of normal force, F_n, and sliding velocity, v_g, which fall below the line A1-S, in region I (see Figure 1), the lubrication condition is characterized by a coefficient of friction of about 0,1 and a specific wear rate of 10^{-2} mm^3/(N·m) to 10^{-6} mm^3/(N·m), i.e. volume wear per unit of normal force, per unit of sliding distance.

If, with v_g not above a value according to point S, the load is increased into region II, a transition into a second condition of lubrication occurs. This mild wear lubrication condition is characterized by a coefficient of friction of about 0,3 to 0,4 and a specific wear rate of 1 mm^3/(N·m) to 5 mm^3/(N·m).

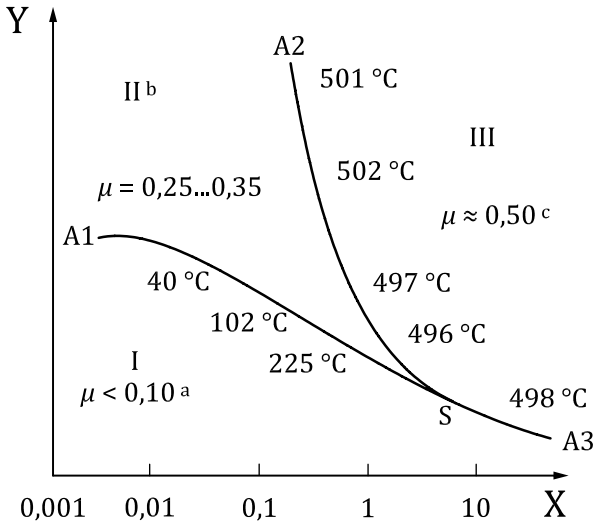

Key

X sliding velocity, v_g, in m/s

Y normal force, F_n

a "No wear" or extremely mild wear.

b Mild wear.

c Scuffing — severe wear.

Figure 1 — Transition diagram for contraform contacts with example of calculated contact temperatures

If load is further increased, a transition into a third condition of lubrication, region III, occurs at intersection of the line A2-S. This region is characterized by a coefficient of friction equal to 0,4 to 0,5. The wear rate, however, is considerably higher, i.e. 100 $mm^3/(N·m)$ to 1 000 $mm^3/(N·m)$, than in regions I and II, and the worn surfaces show evidence of severe wear in the form of scuffing. If load increases at sliding velocities beyond point S, a direct transition from region I to region III takes place.

There is strong evidence that the position of the line A1-S-A3 depends upon lubricant viscosity[20] as well as upon Hertzian contact pressure[16][17]. At combinations of F_n and v_g that fall below this line, the surfaces are kept apart by a thin lubricant film which is, however, penetrated by roughness asperities. In this context, the term "partial elastohydrodynamic lubrication" is used[17].

In region III, liquid film effects are completely absent. This region is identical to the region of "incipient scuffing"[21]. There is evidence that the transition which occurs at intersecting the line A2-S is associated with reaching a critical value of the contact temperature. This is the fundamental concept according to References [8],[9],[10],[11],[12],[13],[14] and [15].

The transition diagram shown is applicable to newly assembled, i.e. unoxidized steel contacts, as occur in gears, cams and followers. It has been found that the diagram is applicable to four-ball as well as to pin-and-ring test results.

Along curve A1-S to A3, the temperature ranges from an oil bath, overall bulk and interfacial bulk temperature of 28 °C at v_g = 0,001 m/s to a contact temperature of 498 °C at v_g = 10 m/s. This temperature behaviour strongly suggests that the collapse of (partial) elasto-hydrodynamical lubrication does not occur at a constant contact or interfacial bulk temperature, for instance, being associated with melting of chemisorbed material. Instead, the pronounced decrease of load carrying capacity with increasing sliding velocity is supposed to be due to decreasing viscosity[20][22][23][24][25].

Contrary to the above, calculated contact temperatures along curve A2-S to A3 tend to attain a constant value, e.g. in the case of AISI 52100[18][20], steel specimens are approximately 500 °C (see Figure 1). This suggests that the II-III transition is associated with a transformation in the steel, causing the

wear mechanism of surfaces to change from mildly adhesive to severely adhesive, perhaps involving a mechanism of thermo-elastic instability[26][27].

Therefore, the results indicate scuffing is associated with a critical magnitude of the contact temperature. For steel lubricated with mineral oils, the critical magnitude does not depend on load, velocity and geometry, and equals near 500 °C.

4.3 Friction at incipient scuffing

As shown in the transition diagram in Figure 1, in the case of scuffing, the coefficient of friction increases from about 0,25 to about 0,5. The corresponding contact temperature proves to be about 500 °C. This contact temperature is the sum of a measured interfacial bulk temperature of 28 °C and a calculated flash temperature of 470 °C. During the flash temperature calculation, the coefficient of friction just before transition, μ = 0,35 is used. If this method has to be applied not only for pin-and-ring tests but also (during the design stage) for gear transmissions, the choice of the value of the critical magnitude of the contact temperature shall be agreed on one hand and the value of the coefficient of friction to be used in the calculations on the other.

A gear load capacity can be predicted

— on the safe side, with the coefficient of friction of μ = 0,50,

— accurately, with the coefficient of friction between μ = 0,25 and μ = 0,35, dependent on the lubricant, and

— according to previous practice, with a low coefficient of friction of regular working conditions, provided that the limiting contact temperature is correspondingly low.

In terms of previous practice, for non-additive and low-additive mineral oils, each combination of oil and rolling materials has a critical scuffing temperature which, in general, is constant regardless of the operating conditions, load, velocity and geometry.

For high-additive and certain kinds of synthetic lubricants, the critical scuffing temperature can well vary from one set of operating conditions to another. So, this critical temperature shall then be determined for each such set separately from tests which closely simulate the operating condition of the gearset.

5 Basic formulae

5.1 Contact temperature

As mentioned in the introduction, the contact temperature is the sum of the interfacial bulk temperature, Θ_{Mi}, (see 5.4) and the flash temperature, Θ_{fl}, (see 5.2), as shown in Formula (1):

$$\Theta_B = \Theta_{Mi} + \Theta_{fl} \quad (1)$$

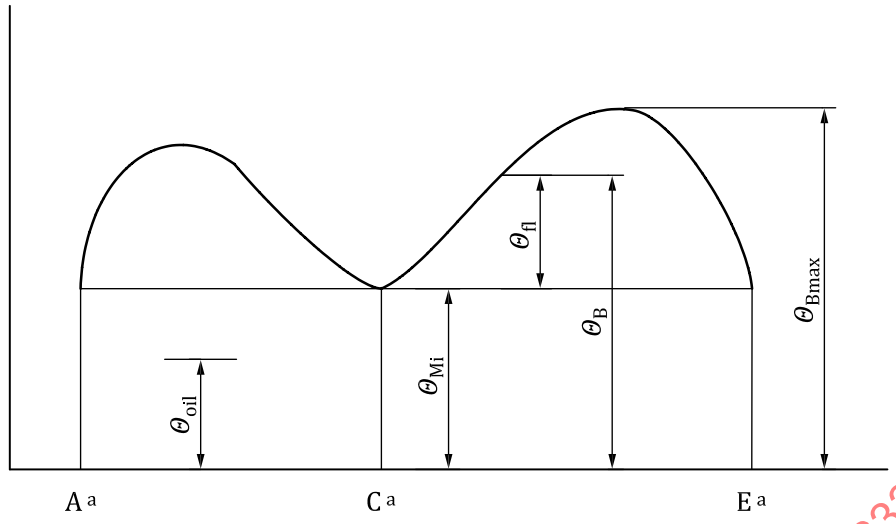

Key

a Position on the path of contact.

Figure 2 — Contact temperature along the path of contact

Only the flash temperature varies along the path of contact (see Figure 2).

The maximum contact temperature is calculated in Formula (2):

$$\Theta_{Bmax} = \Theta_{Mi} + \Theta_{flmax} \tag{2}$$

where Θ_{flmax} is the maximum value of Θ_{fl}, being located either at the approach path or at the recess path.

Prediction of the probability of scuffing is possible by comparing the calculated maximum contact temperature with a critical magnitude. This critical magnitude of the contact temperature can be evaluated from any gear scuffing test or can be provided by field investigations.

For a reliable evaluation of the scuffing risk, it is important that an accurate value of the gear bulk temperature be used for the analysis.

5.2 Flash temperature formula

The flash temperature formula of Blok[8][10][12][28] in a most general representation, for an approximately band-shaped contact and tangential velocities differently directed, see Annex A, is calculated according to Formula (3):

$$\Theta_{fl} = 1{,}11 \cdot \frac{\mu_m \cdot X_\Gamma \cdot X_J \cdot w_{Bn}}{\sqrt{(2 \cdot b_H)}} \cdot \frac{\left|v_{g1} - v_{g2}\right|}{B_{M1} \cdot \sqrt{(v_{g1} \cdot \sin\gamma_1)} + B_{M2} \cdot \sqrt{(v_{g2} \cdot \sin\gamma_2)}} \tag{3}$$

For cylindrical gears, with band-shaped contact and parallel tangential velocities, the general representation (see Annex A) is given in Formula (4):

$$\Theta_{fl} = 1{,}11 \cdot \frac{\mu_m \cdot X_\Gamma \cdot X_J \cdot w_{Bn}}{\sqrt{2 \cdot b_H}} \cdot \frac{\left|v_{g1} - v_{g2}\right|}{B_{M1} \cdot \sqrt{v_{g1}} + B_{M2} \cdot \sqrt{v_{g2}}} \tag{4}$$

or, in an equivalent representation, as shown in Formula (5):

$$\Theta_{\mathrm{fl}} = 2{,}52 \cdot \mu_{\mathrm{m}} \cdot \frac{X_{\mathrm{M}}}{50} \cdot X_{\mathrm{J}} \cdot (X_{\Gamma} \cdot w_{\mathrm{Bt}})^{0{,}75} \cdot \sqrt{\left(\frac{n_1}{60}\right)} \cdot \frac{\left|\sqrt{\rho_{\mathrm{y1}}} - \sqrt{\rho_{\mathrm{y2}} / u}\right|}{\rho_{\mathrm{rely}}^{0{,}25}} \tag{5}$$

where

μ_{m} is the mean coefficient of friction (see Clause 6);

X_{M} is the thermo-elastic factor (see Annex A);

X_{M} = 50 $\mathrm{K \cdot N^{-3/4} \cdot s^{1/2} \cdot m^{-1/2} \cdot mm}$ for commonly applied steel;

X_{J} is the approach factor (see Clause 8);

X_{Γ} is the load sharing factor (see Clause 9);

w_{Bt} is the transverse unit load (see 5.3), in N/mm;

n_1 is the revolutions per minute of pinion, in $\mathrm{min^{-1}}$;

ρ_{rely} is the local relative radius of curvature, in mm, as calculated in Formula (6):

$$\rho_{\mathrm{rely}} = \frac{\rho_{\mathrm{y1}} \cdot \rho_{\mathrm{y2}}}{\rho_{\mathrm{y1}} + \rho_{\mathrm{y2}}} \tag{6}$$

ρ_{y1} is the local radius of curvature of pinion flank, in mm, as calculated in Formula (7):

$$\rho_{\mathrm{y1}} = \frac{1 + \Gamma_{\mathrm{y}}}{1 + u} \cdot a \cdot \sin\alpha_{\mathrm{wt}} \tag{7}$$

ρ_{y2} is the local radius of curvature of wheel flank, in mm, as calculated in Formula (8):

$$\rho_{\mathrm{y2}} = \frac{u - \Gamma_{\mathrm{y}}}{1 + u} \cdot a \cdot \sin\alpha_{\mathrm{wt}} \tag{8}$$

For an adapted representation, see Annex A.

Two Péclet numbers have to be sufficiently high, which is satisfied in almost all cases where scuffing can occur. For lower Péclet numbers, the heat flow from the contact band into the gear teeth causes a different temperature distribution for which Formulae (3) to (6) are not valid.

$$Pé_1 = \frac{v_{\mathrm{g1}} \cdot b_{\mathrm{H}} \cdot \rho_{\mathrm{M1}} \cdot c_{\mathrm{M1}}}{\lambda_{\mathrm{M1}} \cdot \sin\gamma_1} > 5 \tag{9}$$

$$Pé_2 = \frac{v_{\mathrm{g2}} \cdot b_{\mathrm{H}} \cdot \rho_{\mathrm{M2}} \cdot c_{\mathrm{M2}}}{\lambda_{\mathrm{M2}} \cdot \sin\gamma_2} > 5 \tag{10}$$

where

ρ_{M1} is the density of pinion material, in $\mathrm{kg/m^3}$;

ρ_{M2} is the density of wheel material, in $\mathrm{kg/m^3}$;

c_{M1} is the specific heat per unit mass of pinion, in J/(kg·K);

c_{M2} is the specific heat per unit mass of wheel, in J/(kg·K);

λ_{M1} is the heat conductivity of pinion, in N/(s·K);

λ_{M2} is the heat conductivity of wheel, in N/(s·K).

For cylindrical gears, $\sin \gamma_1 = \sin \gamma_2 = 1$.

5.3 Transverse unit load

The transverse unit load for cylindrical gears is calculated in Formula (11):

$$w_{Bt} = K_A \cdot K_v \cdot K_{B\beta} \cdot K_{B\alpha} \cdot K_{mp} \cdot \frac{F_t}{b} \quad (11)$$

where

F_t is the nominal tangential force on pitch circle, in N;

b is the facewidth, in mm;

K_A is the application factor (in accordance with ISO 6336-1);

K_v is the dynamic factor (in accordance with ISO 6336-1);

$K_{B\beta}$ is the face load factor, as shown in Formula (12):

$$K_{B\beta} = K_{H\beta} \text{ (in accordance with ISO 6336-1)} \quad (12)$$

$K_{B\alpha}$ is the transverse load factor, as shown in Formula (13):

$$K_{B\alpha} = K_{H\alpha} \text{ (in accordance with ISO 6336-1)} \quad (13)$$

K_{mp} is the multiple-path factor.

The multiple-path factor, K_{mp}, accounts for the maldistribution in multiple-path transmissions depending on accuracy and flexibility of the branches. If no relevant analysis is available, the following may apply:

— for epicyclical gear trains with n_p planets ($n_p \geq 3$), as shown in Formula (14):

$$K_{mp} = 1 + 0{,}25 \cdot \sqrt{n_p - 3} \quad (14)$$

— for dual tandem gears with quill shaft twist, Φ, degrees under full load, as shown in Formula (15):

$$K_{mp} = 1 + \left(\frac{0{,}2}{\phi} \right) \quad (15)$$

— for double helical gears with an external axial force, F_{ex}, as shown in Formula (16):

$$K_{mp} = 1 + \frac{F_{ex}}{F_t \cdot \tan \beta} \quad (16)$$

— for other cases, as shown in Formula (17):

$$K_{mp} = 1 \quad (17)$$

5.4 Distribution of overall bulk temperatures

The friction loss most typical of gear transmissions is the one caused by the meshing zone. In this source, the heat is generated mainly by tooth friction. The mechanical "pumping" energy expended for sideways expulsion of superfluous oil can sometimes be far from negligible. The other unavoidable friction loss is from the bearings, either of the rolling or the sliding type. In high-speed gear transmissions, sliding bearings can generate much more frictional heat than gears. Other heat sources are oil churning and friction from seals. All the above heat sources have the following features in common:

— in each of these sources, the fluid friction depends on some oil viscosity representative of the operating condition;

— all of the heat sources are thermally interconnected through transmission elements to the sinks, such as the ambient air or the cooling system.

The thermal interconnection allows calculation concepts such as:

— finite element methods for discrete components;

— bondgraph methods;

— thermal network analogue methods[14].

The interfacial bulk temperature, Θ_{Mi}, may be suitably averaged from the two overall bulk temperatures of the teeth in contact, Θ_{M1} and Θ_{M2}. Formula (18) is valid to a good approximation (at high values of the Péclet numbers):

$$\Theta_{Mi} = \frac{B_{M1} \cdot \sqrt{v_{g1}} \cdot \Theta_{M1} + B_{M2} \cdot \sqrt{v_{g2}} \cdot \Theta_{M2}}{B_{M1} \cdot \sqrt{v_{g1}} + B_{M2} \cdot \sqrt{v_{g2}}} \tag{18}$$

In a fairly wide range of the ratio $\frac{B_{M1} \cdot \sqrt{v_{g1}}}{B_{M2} \cdot \sqrt{v_{g2}}}$, a simple arithmetic average is valid to a reasonable approximation in Formula (19):

$$\Theta_{Mi} = \frac{1}{2} \cdot (\Theta_{M1} + \Theta_{M2}) \tag{19}$$

Bulk temperatures in excess of 150 °C for long periods can have an adverse effect on the surface durability.

5.5 Rough approximation of a bulk temperature

For very rough inquiry, the bulk temperature may be estimated by the sum of the oil temperature, taking into account some impediment in heat transfer for spray lubrication, and a part which depends mainly on the flash temperature, of which the maximum value is taken.

$$\Theta_M = \Theta_{oil} + 0,47 \cdot X_S \cdot X_{mp} \cdot \Theta_{flm} \tag{20}$$

where

X_S is 1,2 for spray lubrication;

X_S is 1,0 for dip lubrication;

X_S is 1,0 for meshes with additional spray for cooling purpose;

X_S is 0,2 for gears submerged in oil, provided sufficient cooling;

$$X_{mp} = \frac{1+n_p}{2} \text{ for a pinion with } n_p \text{ mating gears} \quad (21)$$

Θ_{flm} is the average of flash temperature along path of contact, in °C, calculated as Formula (22):

$$\Theta_{flm} = \frac{\int_A^E \Theta_{fl} \cdot d\Gamma_y}{\Gamma_E - \Gamma_A} \quad (22)$$

However, for a reliable evaluation of the scuffing risk, it is important that instead of a rough approximation, an accurate value of the gear bulk temperature be used for the analysis.

6 Coefficient of friction

6.1 General

Several factors influencing the friction between gear teeth vary throughout a meshing cycle. On one of the two mating tooth faces, the relative motion is uniformly accelerating, on the other, it is uniformly decelerating. Only at pitch point position pure rolling occurs. In any other meshing position, combined rolling and sliding will occur. Also, the load acting on two mating tooth faces will vary from one meshing position to another. These conditions cause a continuous variation of the film thickness, the lubrication regime and the coefficient of friction. Even in a similar meshing position, the coefficient of friction can vary for different teeth and different time.

The local coefficient of friction is considered to be a representative quantity valid for the local point concerned, smoothing various influences. The geometrically determined variation of the local coefficient of friction is difficult to calculate or to measure, hence, instead of a local value, a representative mean value of the coefficient of friction will be applied.

A mean value (along the path of contact) of the coefficient of friction has commonly been applied, and even that value is uncertain. Too often, in test reports on friction, important influential quantities were neglected, for instance, the bulk temperature which determines the inlet viscosity and therefore, the lubrication regime.

The mean coefficient of friction, μ_m, depends on the geometry of the path of contact, the tangential velocities, the normal load, the inlet viscosity (which is identical with viscosity at teeth bulk temperature), the pressure viscosity coefficient, the reduced modulus of elasticity, the surface roughness and the normal relative radius of curvature.

NOTE The mean coefficient of friction is defined as the mean value of the local coefficients of friction along the path of contact. Although the actual local coefficient of friction at the pitch point will differ from the mean coefficient of friction defined for the whole path of contact, that mean coefficient of friction can be expressed in terms related to the pitch point.

Depending on further investigations, other quantities and influences shall be accounted for, either in the formula or in the description of the field of application. The number of quantities may be reduced by dimension analysis[29], and a possible neglect of some minor influential quantities.

The coefficient of friction may be measured or estimated according to various methods. The limiting contact temperature shall be chosen correspondingly to the coefficient of friction.

6.2 Mean coefficient of friction, method A

The coefficient of friction at the onset of scuffing may be measured in gear tests or pin-and-ring tests. The limiting contact temperature is correspondingly high.

6.3 Mean coefficient of friction, method B

According to previous practice, whereby low coefficients of friction of regular working conditions are used, the final calculation of the coefficient of friction may be made with some appropriate formula, i.e. one containing a value of absolute (dynamic) viscosity, η_L, that corresponds to the gear bulk temperature. The limiting contact temperature is correspondingly low (see Clause 10).

6.4 Mean coefficient of friction, method C

If at the start of a calculation the bulk temperature is not yet known, the mean coefficient of friction of common working conditions can be estimated by Formula (23):

$$\mu_m = 0{,}060 \cdot \left(\frac{w_{Bt}}{v_{g\Sigma C} \cdot \rho_{relC}} \right)^{0,2} \cdot X_L \cdot X_R \tag{23}$$

where

w_{Bt} is the transverse unit load [see Formula (11)], in N/mm;

$v_{g\Sigma C}$ is the sum of tangential velocities at the pitch point, in m/s, as shown in Formula (24):

$$v_{g\Sigma C} = 2 \cdot v_t \cdot \sin\alpha_{wt} \tag{24}$$

v_t is the pitch line velocity, in m/s (if v_t > 50 m/s, substitute the value 50 in Formula (24), instead of v_t);

ρ_{relC} is the transverse relative radius of curvature, in mm (see Formula (6) for Γ_y = 0);

X_L is the lubricant factor computed in Formula (25):

$$X_L = 1{,}0 \cdot (\eta_{oil})^{-0,05} \text{ for mineral oils;}$$

$$X_L = 0{,}6 \cdot (\eta_{oil})^{-0,05} \text{ for water soluble polyglcols;}$$

$$X_L = 0{,}7 \cdot (\eta_{oil})^{-0,05} \text{ for non-water soluble polyglycols;} \tag{25}$$

$$X_L = 0{,}8 \cdot (\eta_{oil})^{-0,05} \text{ for polyalfaolefins;}$$

$$X_L = 1{,}3 \cdot (\eta_{oil})^{-0,05} \text{ for phosphate esters;}$$

$$X_L = 1{,}5 \cdot (\eta_{oil})^{-0,05} \text{ for traction fluids;}$$

where

η_{oil} is the dynamic viscosity at oil temperature, Θ_{oil}, in mPa·s;

X_R is the roughness factor calculated in Formula (26):

$$X_R = \left(\frac{Ra_1 + Ra_2}{2} \right)^{0,25} \tag{26}$$

where

Ra_1 is the tooth flank surface roughness, Ra, of pinion, for newly manufactured gears, in µm (for adequately run-in gears, Ra_1 can reduce to about 60 % of its initial value);

Ra_2 is the tooth flank surface roughness, Ra, of wheel, for newly manufactured gears, in µm (for adequately run-in gears, Ra_2 can reduce to about 60 % of its initial value).

7 Parameter on the line of action

The points on the line of action are indicated by a dimensionless linear parameter, Γ_y, with the value of −1 in the tangent point on the pinion base circle and the value of 0 in the pitch point[29] (see Figure 3).

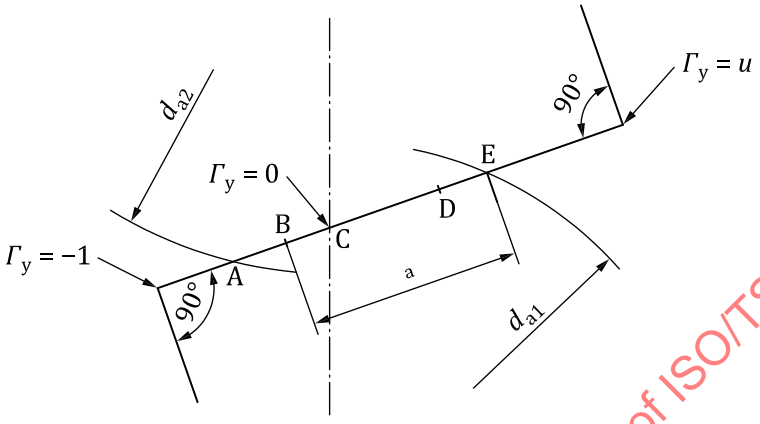

Figure 3 — Parameter on the line of action

At an arbitrary point on the path of contact, see Formula (27):

$$\Gamma_y = \frac{\tan\alpha_{y1}}{\tan\alpha_{wt}} - 1 \tag{27}$$

At the lower end point of the path of contact, see Formula (28):

$$\Gamma_A = -\frac{z_2}{z_1} \cdot \left(\frac{\tan\alpha_{a2}}{\tan\alpha_{wt}} - 1 \right) \tag{28}$$

At the lower point of single pair tooth contact, see Formula (29):

$$\Gamma_B = \frac{\tan\alpha_{a1}}{\tan\alpha_{wt}} - 1 - \frac{2 \cdot \pi}{z_1 \cdot \tan\alpha_{wt}} \tag{29}$$

At the upper point of single pair tooth contact, see Formula (30):

$$\Gamma_D = -\frac{z_2}{z_1} \cdot \left(\frac{\tan\alpha_2}{\tan\alpha_{wt}} - 1 \right) + \frac{2 \cdot \pi}{z_1 \cdot \tan\alpha_{wt}} = \Gamma_A + \frac{2 \cdot \pi}{z_1 \cdot \tan\alpha_{wt}} \tag{30}$$

At the upper end point of the path of contact, see Formula (31):

$$\Gamma_E = \frac{\tan\alpha_{a1}}{\tan\alpha_{wt}} - 1 \tag{31}$$

where the tip pressure angles are defined by Formulae (32) and (33):

$$\tan\alpha_{a1} = \sqrt{\left(\frac{d_{a1}}{d_1 \cdot \cos\alpha_t} \right)^2 - 1} \tag{32}$$

$$\tan\alpha_{a2} = \sqrt{\left(\frac{d_{a2}}{d_2 \cdot \cos\alpha_t}\right)^2 - 1} \tag{33}$$

8 Approach factor

The approach factor takes empirically into account an increased scuffing risk in the beginning of the approach path, due to mesh starting without any previously built up oil film. Its influence is relatively strong for large gears.

The approach factor is,

— if the pinion drives the wheel (speed reducing), as shown in Formulae (34) and (35):

$$X_J = 1 \text{ for } \Gamma_y \geq 0 \tag{34}$$

$$X_J = 1 + \frac{C_{eff} - C_{a2}}{50} \cdot \left(\frac{-\Gamma_y}{\Gamma_E - \Gamma_A}\right)^3 \text{, provided } X_J \geq 1 \text{ for } \Gamma_y < 0 \tag{35}$$

— if the wheel drives the pinion (speed increasing), as shown in Formulae (36) and (37):

$$X_J = 1 \text{ for } \Gamma_y \leq 0 \tag{36}$$

$$X_J = 1 + \frac{C_{eff} - C_{a1}}{50} \cdot \left(\frac{\Gamma_y}{\Gamma_E - \Gamma_A}\right)^3 \text{ provided } X_J \geq 1 \text{ for } \Gamma_y > 0 \tag{37}$$

where

C_{eff} is the optimal tip relief (see Annex B), in µm;

C_{a1} is the tip relief of pinion, in µm;

C_{a2} is the tip relief of wheel, in µm;

Γ_y is the parameter of arbitrary point (see Clause 7);

Γ_A is the parameter of point A (see Clause 7);

Γ_E is the parameter of point B (see Clause 7).

9 Load sharing factor, X_Γ

9.1 General

The load sharing factor, X_Γ, accounts for the load sharing of succeeding pairs of meshing teeth. The load sharing factor is presented as a function of the linear parameter, Γ_y, on the path of contact[37].

Due to inaccuracies, a preceding pair of meshing teeth can cause an instantaneous increase or decrease of the theoretical load sharing factor, independent of the instantaneous increase or decrease caused by inaccuracies of a succeeding pair of meshing teeth at a later time. The value of X_Γ does not exceed 1,0 (for cylindrical gears), which means full transverse single tooth contact. The region of transverse single tooth contact may be extended by an irregularly varying location of a dynamic load.

The load sharing factor, X_Γ, depends on the type of gear transmission and on the profile modification. In case of buttressing of helical teeth (no profile modification), the load sharing factor is combined with a buttressing factor, $X_{but,\Gamma}$[37].

9.2 Spur gears with unmodified profiles

The load sharing factor for a spur gear with unmodified profile is conventionally supposed to have a discontinuous trapezoidal shape (see Figure 4). However, due to manufacturing inaccuracies, in each path of double contact, the load sharing factor will increase for protruding flanks and decrease for other flanks. The representative load sharing factor is an envelope of possible curves (see Figure 5).

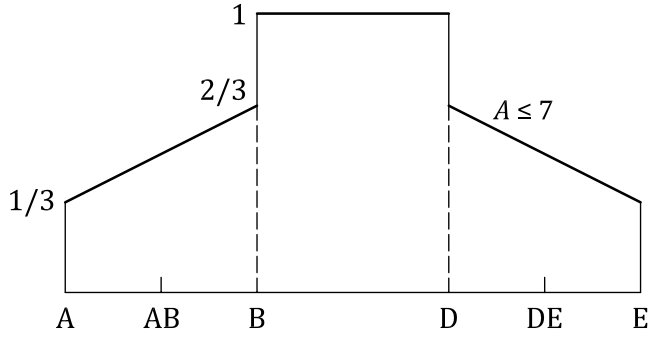

Figure 4 — Load sharing factor for cylindrical spur gears with unmodified profiles and tolerance class A ≤ 7

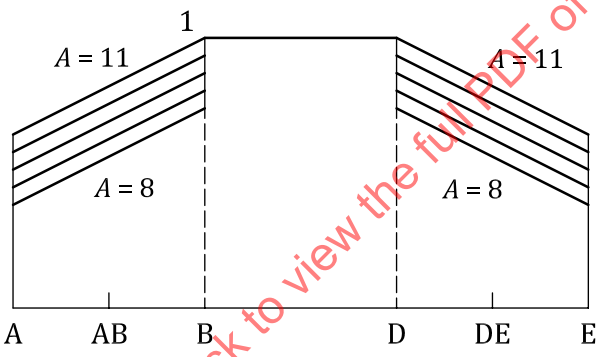

Figure 5 — Load sharing factor for cylindrical spur gears with unmodified profiles and tolerance class 8 ≤ A ≤ 11

$$X_\Gamma = \frac{A-3}{12} + \frac{1}{3}\cdot\frac{\Gamma_y - \Gamma_A}{\Gamma_B - \Gamma_A} \quad \text{for } \Gamma_A \le \Gamma_y < \Gamma_B \tag{38}$$

$$X_\Gamma = 1{,}0 \quad \text{for } \Gamma_B \le \Gamma_y \le \Gamma_D \tag{39}$$

$$X_\Gamma = \frac{A-3}{12} + \frac{1}{3}\cdot\frac{\Gamma_E - \Gamma_y}{\Gamma_E - \Gamma_D} \quad \text{for } \Gamma_D < \Gamma_y \le \Gamma_B \tag{40}$$

where

A is 7 for tolerance class ≤ 7, in accordance with ISO 1328-1;

A is the tolerance class for class ≥ 8, in accordance with ISO 1328-1.

9.3 Spur gears with profile modification

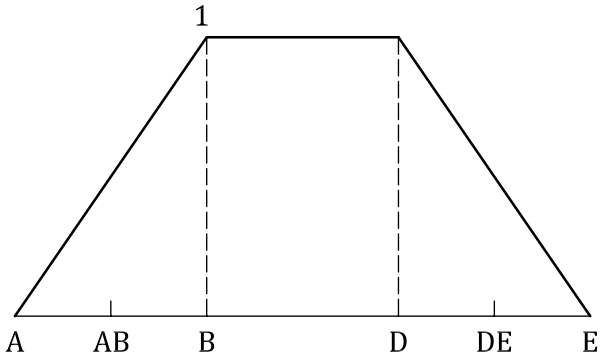

Figure 6 — Load sharing factor for cylindrical spur gears with adequate profile modification on pinion and wheel

$$X_\Gamma = \frac{\Gamma_y - \Gamma_A}{\Gamma_B - \Gamma_A} \qquad \text{for } \Gamma_A \le \Gamma_y \le \Gamma_B \tag{41}$$

$$X_\Gamma = 1{,}0 \qquad \text{for } \Gamma_B < \Gamma_y < \Gamma_D \tag{42}$$

$$X_\Gamma = \frac{\Gamma_E - \Gamma_y}{\Gamma_E - \Gamma_D} \qquad \text{for } \Gamma_D \le \Gamma_y \le \Gamma_E \tag{43}$$

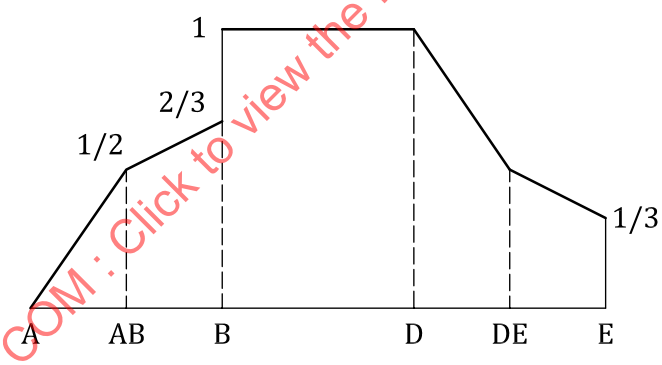

Figure 7 — Load sharing factor for cylindrical spur gears with adequate profile modification on the addendum of the wheel and/or the dedendum of the pinion

$$X_\Gamma = \frac{\Gamma_y - \Gamma_A}{\Gamma_B - \Gamma_A} \qquad \text{for } \Gamma_A \le \Gamma_y \le \Gamma_{AB} \tag{44}$$

$$X_\Gamma = \frac{1}{3} + \frac{1}{3} \cdot \frac{\Gamma_y - \Gamma_A}{\Gamma_B - \Gamma_A} \qquad \text{for } \Gamma_{AB} < \Gamma_y < \Gamma_B \tag{45}$$

$$X_\Gamma = 1{,}0 \qquad \text{for } \Gamma_B \le \Gamma_y < \Gamma_D \tag{46}$$

$$X_\Gamma = \frac{\Gamma_E - \Gamma_y}{\Gamma_E - \Gamma_D} \qquad \text{for } \Gamma_D \le \Gamma_y \le \Gamma_{DE} \tag{47}$$

$$X_\Gamma = \frac{1}{3} + \frac{1}{3} \cdot \frac{\Gamma_E - \Gamma_y}{\Gamma_E - \Gamma_D} \qquad \text{for } \Gamma_{DE} < \Gamma_y \le \Gamma_E \tag{48}$$

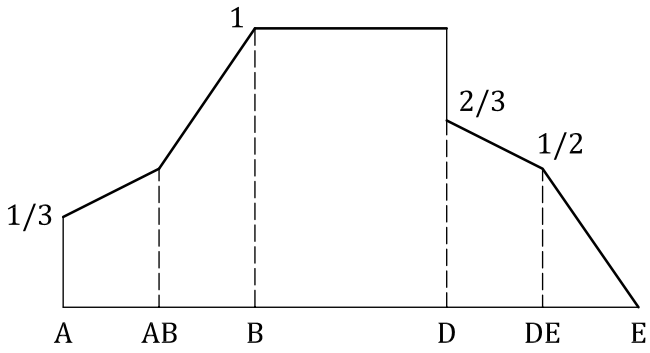

Figure 8 — Load sharing factor for cylindrical spur gears with adequate profile modification on the addendum of the pinion and/or the dedendum of the wheel

$$X_\Gamma = \frac{1}{3} + \frac{1}{3} \cdot \frac{\Gamma_y - \Gamma_A}{\Gamma_B - \Gamma_A} \qquad \text{for } \Gamma_A \le \Gamma_y \le \Gamma_{AB} \tag{49}$$

$$X_\Gamma = \frac{\Gamma_y - \Gamma_A}{\Gamma_B - \Gamma_A} \qquad \text{for } \Gamma_{AB} \le \Gamma_y \le \Gamma_B \tag{50}$$

$$X_\Gamma = 1{,}0 \qquad \text{for } \Gamma_B < \Gamma_y < \Gamma_D \tag{51}$$

$$X_\Gamma = \frac{1}{3} + \frac{1}{3} \cdot \frac{\Gamma_E - \Gamma_y}{\Gamma_E - \Gamma_D} \qquad \text{for } \Gamma_D < \Gamma_y \le \Gamma_{DE} \tag{52}$$

$$X_\Gamma = \frac{\Gamma_E - \Gamma_y}{\Gamma_E - \Gamma_D} \qquad \text{for } \Gamma_{DE} < \Gamma_y \le \Gamma_E \tag{53}$$

9.4 Buttressing factor, $X_{but,\Gamma}$

Helical gears can have a buttressing effect near the end points A and E of the path of contact, due to the oblique contact lines. This applies to cylindrical helical gears with no profile modification.

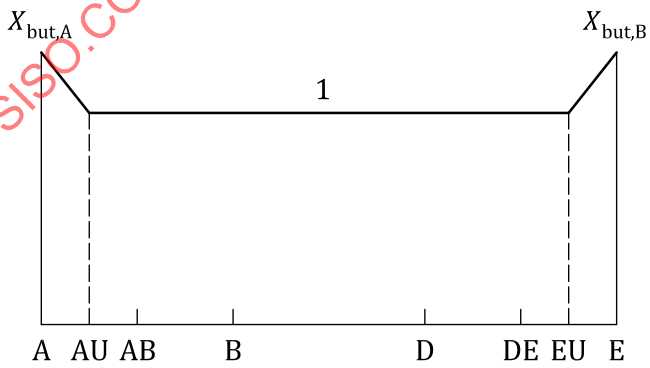

Figure 9 — Buttressing factor, $X_{but,\Gamma}$

The buttressing is expressed by means of a factor, $X_{\mathrm{but},\Gamma}$ (see Figure 9), marked by the following values in Formulae (54):

$$\Gamma_{\mathrm{AU}} - \Gamma_{\mathrm{A}} = \Gamma_{\mathrm{E}} - \Gamma_{\mathrm{EU}} = 0{,}2 \text{ mm} \cdot \sin\beta_{\mathrm{b}} \tag{54}$$

with

$$X_{\mathrm{but,A}} = X_{\mathrm{but,E}} = 1{,}3 \qquad \text{if } \varepsilon_\beta \geq 1{,}0 \tag{55}$$

$$X_{\mathrm{but,A}} = X_{\mathrm{but,E}} = 1 + 0{,}3 \cdot \varepsilon_\beta \qquad \text{if } \varepsilon_\beta < 1{,}0 \tag{56}$$

$$X_{\mathrm{but,AU}} = X_{\mathrm{but,EU}} = 1{,}0 \tag{57}$$

$$X_{\mathrm{but},\Gamma} = X_{\mathrm{but,A}} - \frac{\Gamma_{\mathrm{y}} - \Gamma_{\mathrm{A}}}{\Gamma_{\mathrm{AU}} - \Gamma_{\mathrm{A}}} \cdot \left(X_{\mathrm{but,A}} - 1\right) \qquad \text{for } \Gamma_{\mathrm{A}} \leq \Gamma_{\mathrm{y}} < \Gamma_{\mathrm{AU}} \tag{58}$$

$$X_{\mathrm{but},\Gamma} = 1{,}0 \qquad \text{for } \Gamma_{\mathrm{AU}} \leq \Gamma_{\mathrm{y}} \leq \Gamma_{\mathrm{EU}} \tag{59}$$

$$X_{\mathrm{but},\Gamma} = X_{\mathrm{but,E}} - \frac{\Gamma_{\mathrm{E}} - \Gamma_{\mathrm{y}}}{\Gamma_{\mathrm{E}} - \Gamma_{\mathrm{EU}}} \cdot \left(X_{\mathrm{but,E}} - 1\right) \qquad \text{for } \Gamma_{\mathrm{EU}} < \Gamma_{\mathrm{y}} \leq \Gamma_{\mathrm{E}} \tag{60}$$

where ε_β is the overlap ratio.

9.5 Helical gears with $\varepsilon_\beta \leq 0{,}8$ and unmodified profiles

Helical gears with a contact ratio $\varepsilon_\alpha \geq 1$ and overlap ratio $\varepsilon_\beta \leq 0{,}8$ still have poor single contact of tooth pairs. Hence, they can be treated similar to spur gears, considering the geometry in the transverse plane, as well as the buttressing effect (see Figure 10).

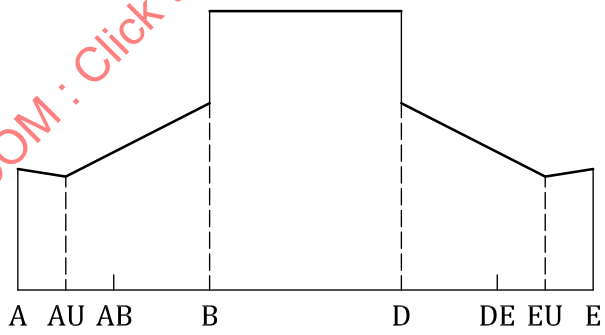

Figure 10 — Load sharing factor for cylindrical helical gears with $\varepsilon_\beta \leq 0{,}8$ and unmodified profiles, including the buttressing effect

The load sharing factor is obtained by multiplying the X_Γ in Clause 9 with the buttressing factor, $X_{\mathrm{but},\Gamma}$, in 9.4.

9.6 Helical gears with $\varepsilon_\beta \leq 0{,}8$ and profile modification

Helical gears with a contact ratio $\varepsilon_\alpha \geq 1$ and overlap ratio $\varepsilon_\beta \leq 0{,}8$ still have poor single contact of tooth pairs. Hence, they can be treated similar to spur gears, considering the geometry in the transverse plane (see Figure 11, Figure 12 and Figure 13).

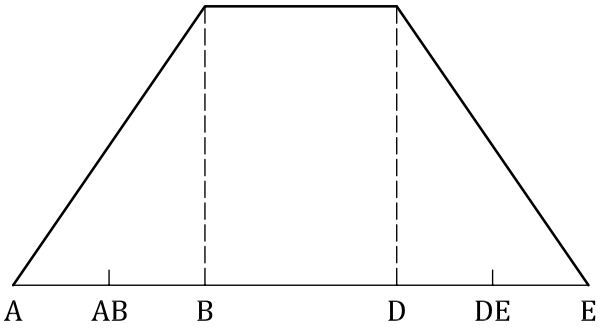

Figure 11 — Load sharing factor for cylindrical helical gears with $\varepsilon_\beta \leq 0{,}8$ and adequate profile modification

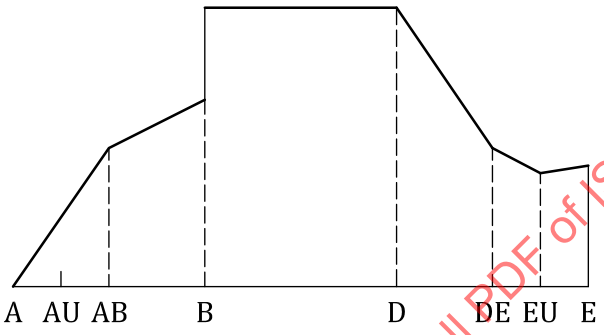

Figure 12 — Load sharing factor for cylindrical helical gears with $\varepsilon_\beta \leq 0{,}8$ and adequate profile modification on the addendum of the wheel and/or the dedendum of the pinion

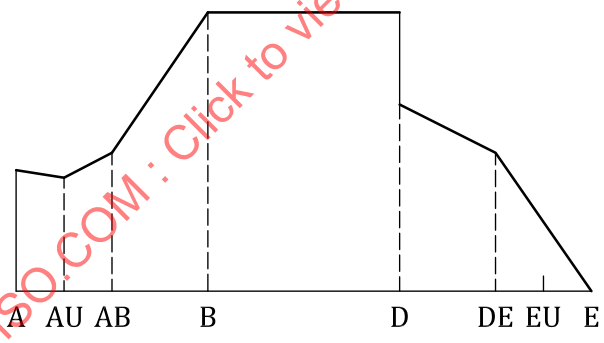

Figure 13 — Load sharing factor for cylindrical helical gears with $\varepsilon_\beta \leq 0{,}8$ and adequate profile modification on the addendum of the pinion and/or the dedendum of the wheel

The load sharing factor is obtained by multiplying the X_Γ in Clause 9 with the buttressing factor, $X_{\mathrm{but},\Gamma}$, in 9.4.

9.7 Helical gears with $\varepsilon_\beta \geq 1{,}2$ and unmodified profiles

The buttressing effect of local high mesh stiffness at the end of oblique contact lines for helical gears with $\varepsilon_\alpha \geq 1$ and $\varepsilon_\beta \geq 1{,}2$, is assumed to act near the ends A and E along the helix teeth over a constant length, which corresponds to a transverse relative distance of $0{,}2\ \mathrm{mm} \cdot \sin\beta_\mathrm{b}$ (see 9.4 and Figures 9 and 14).

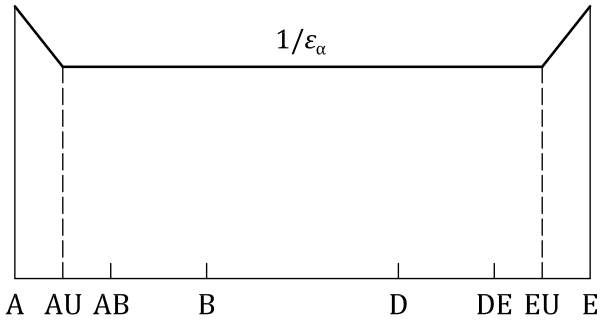

Figure 14 — Load sharing factor for cylindrical helical gears with $\varepsilon_\beta \geq 1$ and unmodified profiles

The load sharing factor is obtained by multiplying the value $1/\varepsilon_\alpha$, representing the mean load, with the buttressing factor, $X_{\mathrm{but},\Gamma}$.

$$X_\Gamma = \frac{1}{\varepsilon_\alpha} \cdot X_{\mathrm{but},\Gamma} \tag{61}$$

where ε_α is the transverse contact ratio.

9.8 Helical gears with $\varepsilon_\beta \geq 1{,}2$ and profile modification

Tip relief on the pinion (respectively wheel) reduces X_Γ in the range DE-E (respectively A-AB) and increases X_Γ in the range AB-DE (see Figure 15, Figure 16 and Figure 17). The extensions of tip relief at both ends A-AB and DE-E of the path of contact are assumed to be equal and to result in a contact ratio $\varepsilon_\alpha = 1$ for unloaded gears (see Figure 15).

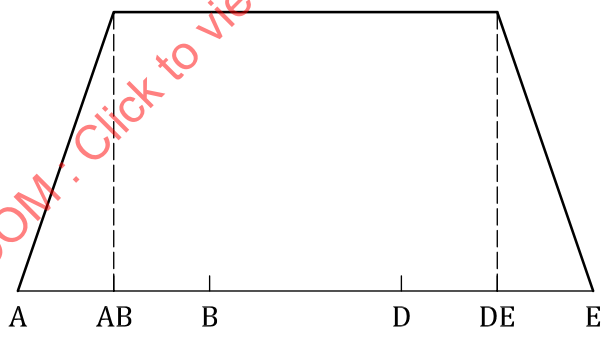

Figure 15 — Load sharing factor for cylindrical helical gears with $\varepsilon_\beta \geq 1{,}2$ and adequate profile modification on pinion and wheel

$$X_\Gamma = \left[\frac{1}{\varepsilon_\alpha} + \frac{(\varepsilon_\alpha - 1)}{\varepsilon_\alpha \cdot (\varepsilon_\alpha + 1)}\right] \cdot \frac{\Gamma_y - \Gamma_A}{\Gamma_{AB} - \Gamma_A} \qquad \text{for } \Gamma_A \leq \Gamma_y \leq \Gamma_{AB} \tag{62}$$

$$X_\Gamma = \frac{1}{\varepsilon_\alpha} + \frac{(\varepsilon_\alpha - 1)}{\varepsilon_\alpha \cdot (\varepsilon_\alpha + 1)} \qquad \text{for } \Gamma_{AB} < \Gamma_y \leq \Gamma_{DE} \tag{63}$$

$$X_\Gamma = \left[\frac{1}{\varepsilon_\alpha} + \frac{(\varepsilon_\alpha - 1)}{\varepsilon_\alpha \cdot (\varepsilon_\alpha + 1)}\right] \cdot \frac{\Gamma_E - \Gamma_y}{\Gamma_E - \Gamma_{DE}} \qquad \text{for } \Gamma_{DE} < \Gamma_y \leq \Gamma_E \tag{64}$$

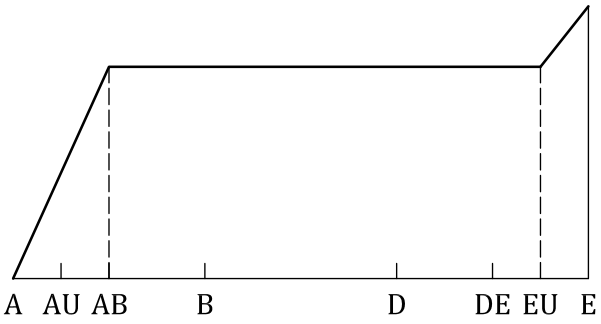

Figure 16 — Load sharing factor for cylindrical helical gears with $\varepsilon_\beta \geq 1{,}2$ and adequate profile modification on the addendum of the wheel and/or the dedendum of the pinion

$$X_\Gamma = \left[\frac{1}{\varepsilon_\alpha} + \frac{(\varepsilon_\alpha - 1)}{2 \cdot \varepsilon_\alpha \cdot (\varepsilon_\alpha + 1)}\right] \cdot \frac{\Gamma_y - \Gamma_A}{\Gamma_{AB} - \Gamma_A} \qquad \text{for } \Gamma_A \leq \Gamma_y \leq \Gamma_{AB} \tag{65}$$

$$X_\Gamma = \frac{1}{\varepsilon_\alpha} + \frac{(\varepsilon_\alpha - 1)}{2 \cdot \varepsilon_\alpha \cdot (\varepsilon_\alpha + 1)} \qquad \text{for } \Gamma_{AB} < \Gamma_y \leq \Gamma_{DE} \tag{66}$$

$$X_\Gamma = \left[\frac{1}{\varepsilon_\alpha} + \frac{(\varepsilon_\alpha - 1)}{2 \cdot \varepsilon_\alpha \cdot (\varepsilon_\alpha + 1)}\right] \cdot X_{\text{but},\Gamma} \qquad \text{for } \Gamma_{DE} < \Gamma_y \leq \Gamma_E \tag{67}$$

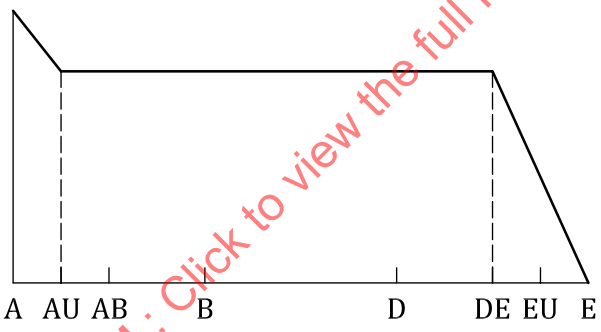

Figure 17 — Load sharing factor for cylindrical helical gears with $\varepsilon_\beta \geq 1{,}2$ and adequate profile modification on the addendum of the pinion and/or the dedendum of the wheel

$$X_\Gamma = \left[\frac{1}{\varepsilon_\alpha} + \frac{(\varepsilon_\alpha - 1)}{2 \cdot \varepsilon_\alpha \cdot (\varepsilon_\alpha + 1)}\right] \cdot X_{\text{but},\Gamma} \qquad \text{for } \Gamma_A \leq \Gamma_y \leq \Gamma_{AB} \tag{68}$$

$$X_\Gamma = \frac{1}{\varepsilon_\alpha} + \frac{(\varepsilon_\alpha - 1)}{2 \cdot \varepsilon_\alpha \cdot (\varepsilon_\alpha + 1)} \qquad \text{for } \Gamma_{AB} < \Gamma_y \leq \Gamma_{DE} \tag{69}$$

$$X_\Gamma = \left[\frac{1}{\varepsilon_\alpha} + \frac{(\varepsilon_\alpha - 1)}{2 \cdot \varepsilon_\alpha \cdot (\varepsilon_\alpha + 1)}\right] \cdot \frac{\Gamma_E - \Gamma_y}{\Gamma_E - \Gamma_{DE}} \qquad \text{for } \Gamma_{DE} < \Gamma_y \leq \Gamma_E \tag{70}$$

9.9 Helical gears with $0{,}8 < \varepsilon_\beta < 1{,}2$

Due to the fact that gears are not infinitely stiff, the overlap ratio changes depending on the load. To take this into account, for helical gears with calculated overlap ratios $0{,}8 < \varepsilon_\beta < 1{,}2$, an interpolation between the load sharing factor $X_\Gamma(\varepsilon_\beta = 0{,}8)$ for $\varepsilon_\beta = 0{,}8$ (see 9.5 for unmodified profiles and 9.6 for modified

profiles) and X_Γ (ε_β = 1,2) for ε_β = 1,2 (see 9.7 for unmodified profiles and 9.8 for modified profiles) shall be performed. For helical gears with 0,8 < ε_β < 1,2, X_Γ is calculated as shown in Formula (71):

$$X_\Gamma(\varepsilon_\beta) = X_\Gamma(\varepsilon_\beta = 0{,}8) \cdot \frac{1{,}2 - \varepsilon_\beta}{0{,}4} + X_\Gamma(\varepsilon_\beta = 1{,}2) \cdot \frac{\varepsilon_\beta - 0{,}8}{0{,}4} \tag{71}$$

10 Scuffing temperature and safety

10.1 Scuffing temperature

The scuffing temperature is the contact temperature at which scuffing is likely to occur with the chosen combination of lubricant and gear materials. The scuffing temperature is assumed to be a characteristic value for the material-lubricant-material system of a gear pair, to be determined by gear tests with the same material-lubricant-material system[31].

When using a low-additive mineral oil, the scuffing temperature is assumed to be independent of operating conditions in a fairly wide range.

When using a mineral oil or a synthetic oil with anti-scuff or friction-reducing additives, extended research is still needed to determine the nature of a possible non-constancy of the scuffing temperature for the materials and the operating conditions concerned. Special attention shall be paid to the correlation between test conditions and actual or design conditions. The correlation can be strongly influenced by properties shown in the transition diagram (see Figure 1).

10.2 Structural factor

The scuffing temperature of low-additive mineral oils that is determined from test gears can be extended to different gear steels, heat treatments or surface treatments by introducing an empirical structural factor, as shown in Formula (72):

$$\Theta_S = \Theta_{MT} + X_W \cdot \Theta_{flmaxT} \tag{72}$$

where

Θ_{MT} is the bulk temperature of test gears, in °C;

Θ_{flmaxT} is the maximum flash temperature of test gears, in K;

X_W is the structural factor (see Table 3).

Table 3 — Structural factor

Material	X_W
Through hardened steel	1,00
Phosphated steel	1,25
Copper-plated steel	1,50
Bath or gas nitrided steel	1,50
Hardened carburized steel, with austenite content	
— less than average	1,15
— average (10 % to 20 %)	1,00
— greater than average	0,85
Austenite steel (stainless steel)	0,45

However, this approximation is restricted to methods using the coefficient of friction for common working conditions (see 6.4) together with an average value of the thermo-elastic factor (see Clause 8). The structural factor can be unnecessary if methods are used considering realistic values of the coefficient of friction and the thermo-elastic factor.

10.3 Contact exposure time

It was shown by tests[32] that the scuffing temperature of gears lubricated with anti-scuff oils can be influenced by the contact exposure time, that is the time during which a point on a tooth flank is exposed to the Hertzian contact band of the meshing tooth 1.

The decisive contact exposure time, t_{max}, for a pair of tooth flanks is the longest of t_1 and t_2.

$$t_{max} \geq t_1 = \frac{2 \cdot b_H}{v_{g1}} \tag{73}$$

$$t_{max} \geq t_2 = \frac{2 \cdot b_H}{v_{g2}} \tag{74}$$

The dependence of the scuffing temperature, Θ_S, on the contact time is approximated as shown in Figure 18 by a curve consisting of two straight lines.

$$\Theta_S = \Theta_{Sc} + X_\Theta \cdot X_W \cdot (t_c - t_{max}) \qquad \text{for } t_{max} < t_c \tag{75}$$

$$\Theta_S = \Theta_{Sc} \qquad \text{for } t_{max} \geq t_c \tag{76}$$

where

Θ_{Sc} is the scuffing temperature at long contact times, in °C;

X_Θ is the gradient of the scuffing temperature, in K/µs;

X_W is the structural factor;

t_c is the contact exposure time at the bend of the curve, in µs;

t_{max} is the contact exposure time of meshing teeth, in µs.

The following values may be applied for oils:

— without anti-scuff additives: X_Θ = 0 K/µs, t_c = 0 µs;

— with anti-scuff additives: X_Θ = 18 K/µs, t_c = 18 µs.

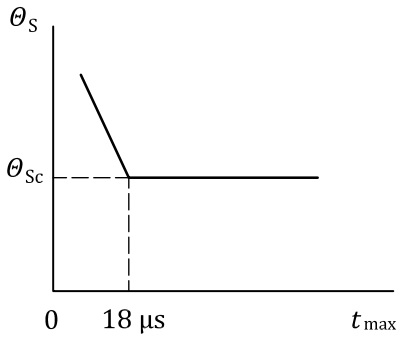

Figure 18 — Influence of contact exposure time on the scuffing temperature for anti-scuff oils

10.4 Scuffing temperature in gear tests

The scuffing temperature can be determined in gear tests, such as Ryder[33], FZG-Ryder[34], FZG L-42, FZG A/8,3/90[35].

The test result shall be expressed in a scuffing temperature, together with the test conditions. If the test result is expressed in other terms, then a relation shall be given as shown in Formula (77):

$$\Theta_S = 80 + (0{,}85 + 1{,}4 \cdot X_W) \cdot X_L \cdot (S_{FZG})^2 \quad (77)$$

where

X_W is the structural factor (see Table 3);

X_L is the lubricant factor, [see Formula (26)];

S_{FZG} is the load stage, according to FZG A/8,3/90 test, where scuffing occurs.

However, oil data tend to vary a lot with regard to S_{FZG}, a load stage variation of ±1 is common, and it is assumed that the oil somewhat deteriorates during an oil shift interval. Therefore, calculations may be made with one load stage less than the specification.

10.5 Safety range

In contrast to the length of time that fatigue damage takes to develop, a single momentary overload can initiate scuffing of such severity that affected gears are no longer be fit for use. This should be carefully considered when choosing an adequate safety range, especially for gears required to operate with high pitch line velocities.

In cases with a short contact exposure time, t_{max}, and safety conditions based on an increased scuffing temperature, $\Theta_S > \Theta_{Sc}$, (see 10.3) that contact exposure time, t_{max}, shall not increase, unless the transmitted power is lowered adequately.

A safety factor may be defined by Formula (78):

$$S_B = \frac{\Theta_S - \Theta_{oil}}{\Theta_{Bmax} - \Theta_{oil}} \quad (78)$$

where

Θ_S scuffing temperature, in °C;

Θ_{Bmax} is the maximum contact temperature, in °C;

Θ_{oil} is the oil temperature, in °C.

However, the relation between the actual gear load and the decisive contact temperature is very complicated, and the use of a safety factor expressed in any quotient of temperatures can cause confusion.

Therefore, in addition to the specification of the test load stage (see 10.4), it is advised to express the concept of safety as a demanded minimum difference (for instance, ≥50 K) between the scuffing temperature and the estimated maximum contact temperature.

Annex A
(informative)

Flash temperature formula presentation

A.1 General

Since the first publication of the original flash temperature (see References [8] and [10]), Blok made the following conversions:

— step from width to semi-width of Hertzian contact band and substitution of $0{,}83 \cdot \sqrt{2} = 1{,}17$ for parabolic friction heat distribution by 1,11 for elliptic friction heat distribution[12];

— extension to unequally directed tangential velocities[28] [see Formula (24)].

For convenience, the following exact conversions were made:

— some quantities were expressed in other quantities, for instance, the semi-width of Hertzian contact band and the radii of curvature;

— some parts of the formula were concentrated in separate factors, for instance, the thermo-elastic factor (see A.4).

For practical applications, the following adaptive conversions were made:

— redefinition of factors, for instance, the load sharing factor (see Clause 9);

— addition of empirical factors, for instance, the approach factor (see Clause 8).

A.2 General case

In a most general case of tooth contact, the successive contact areas assume the shape of tapered bands (see Figure A.1). Moreover, the two tangential velocities, v_{g1} and v_{g2}, are directed at unequal angles, γ_1 and γ_2, with respect to the longitudinal axis of such an area. In simpler cases (e.g. cylindrical gears), the angles reduce into $\gamma_1 = \gamma_2 = \pi/2$.

The distribution of the contact pressures over some cross-section in a tapered contact area may be approximated by the semi-elliptical distribution that would occur over a substitute band-shaped contact area interposed between two parallel surfaces, while having a uniform width equal to the aforementioned local width (see Figure A.1).

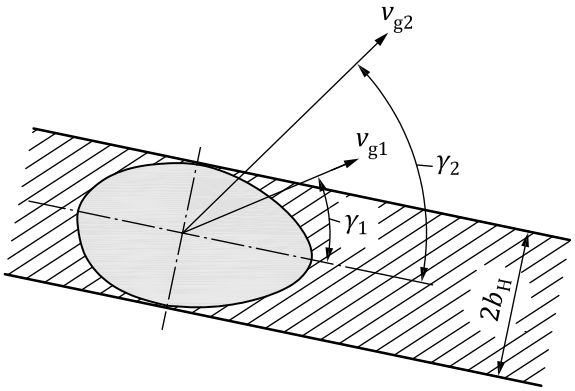

Figure A.1 — Substitute band-shaped contact area, with two tangential velocities in different directions

For determining the maximum flash temperature sought, the actual elliptic contact zone may be substituted by a band-shaped contact zone of which the width, $2b_H$ equals the length of the minor axis of the ellipse (see Figure A.1).

The maximum contact pressure here, like the minor axis, can be directly proportional to the cubic root of the load, instead of the square root. In some cases, the Hertzian formulae shall be adapted for elongated point contact[36].

To summarize, the present procedure appears justifiable to a reasonable approximation. A major reason lies in the feature that, for the actual sufficiently elongated elliptic contacts under the above-defined kinematic conditions, the actual maximum flash temperature can be expected to occur at a point fairly close to the minor axis concerned.

The flash temperature formula of Blok[8][10][12][28] for substitute band-shaped contact and tangential velocities differently directed is:

$$\Theta_{fl} = 1{,}11 \cdot \frac{\mu_m \cdot X_\Gamma \cdot X_J \cdot w_{Bn} \cdot |v_{g1} - v_{g2}|}{\sqrt{2 \cdot b_H} \cdot B_{M1} \cdot \sqrt{v_{g1} \cdot \sin\gamma_1} + B_{M2} \cdot \sqrt{v_{g2} \cdot \sin\gamma_2}} \quad \text{(A.1)}$$

where

μ_m is the mean coefficient of friction;

X_J is the approach factor (see Clause 8);

X_Γ is the load sharing factor (see Clause 9);

w_{Bn} is the normal unit load, in N/mm, as shown in Formula (A.2):

$$w_{Bn} = \frac{w_{Bt}}{\cos\alpha_{wn} \cdot \cos\beta_w} \quad \text{(A.2)}$$

where

w_{Bt} is the transverse unit load (see 5.3), in N/mm;

α_{wn} is the normal working pressure angle, in degrees, as shown in Formula (A.3):

$$\alpha_{wn} = \arcsin(\sin\alpha_{wt} \cdot \cos\beta_b) \quad \text{(A.3)}$$